


Majorana Superconducting Qubit

Constantin Schrade and Liang Fu

Department of Physics, Massachusetts Institute of Technology, 77 Massachusetts Avenue, Cambridge, Massachusetts 02139, USA

 (Received 2 March 2018; published 27 December 2018)

We propose a platform for universal quantum computation that uses conventional s -wave superconducting leads to address a topological qubit stored in spatially separated Majorana bound states in a multiterminal topological superconductor island. Both the manipulation and readout of this “Majorana superconducting qubit” are realized by tunnel couplings between Majorana bound states and the superconducting leads. The ability of turning on and off tunnel couplings on demand by local gates enables individual qubit addressability while avoiding cross-talk errors. By combining the scalability of superconducting qubit and the robustness of topological qubits, the Majorana superconducting qubit may provide a promising and realistic route towards quantum computation.

DOI: [10.1103/PhysRevLett.121.267002](https://doi.org/10.1103/PhysRevLett.121.267002)

Superconducting circuits are among the leading platforms for quantum computing. Their main building block is the superconducting qubit that is based on the Josephson tunnel junction, a nondissipative and nonlinear electrical element that enables long-coherence times [1–3] and high-fidelity gate operations [4,5]. With recent advances in scaling to qubit arrays and surface code architectures [6–11], significant efforts are being made to minimize errors due to unintentional cross talk between qubits [11–14] and to avoid leakage into noncomputational states [15,16].

In this work, we introduce a new platform for universal quantum computing that combines the scalability of the superconducting qubit and the robustness of the Majorana qubit. The key element in our proposal is a multiterminal topological superconductor (TSC) island with spatially separated Majorana bound states (MBSs) used as a weak link between superconducting electrodes. The minimal setup is a Josephson junction that consists of two TSC weak links in parallel within a superconducting loop, as shown in Fig. 1(a). Both TSC islands operate in the Coulomb blockade regime and mediate the Josephson coupling via virtual charge fluctuations. The first island hosts four MBSs ($\gamma_1, \gamma_2, \gamma_3, \gamma_4$) at the four terminals, which stores a single topological qubit. The second is a two-terminal island with two MBSs ($\gamma_{1,\text{ref}}, \gamma_{2,\text{ref}}$) used for qubit manipulation and readout only. The full set of single-qubit rotations is achieved by selectively turning on and off the tunnel couplings between individual MBSs and the SC electrodes that enable different Cooper pair splitting processes, see Figs. 1(b) and 1(c). The qubit readout is achieved by measuring the persistent supercurrent in the loop; see Fig. 1(a). We term this basic building block—a Majorana-based qubit in an all-superconducting circuit—the “Majorana superconducting qubit” (MSQ).

Compared to the conventional superconducting qubit, the MSQ is expected to have several advantages. First, the

nonlocal storage of quantum information in well-separated MBSs makes the MSQ protected from decoherence under local perturbations at a physical level [17]. The MSQ is also insensitive to global electrostatic fluctuations that couple to

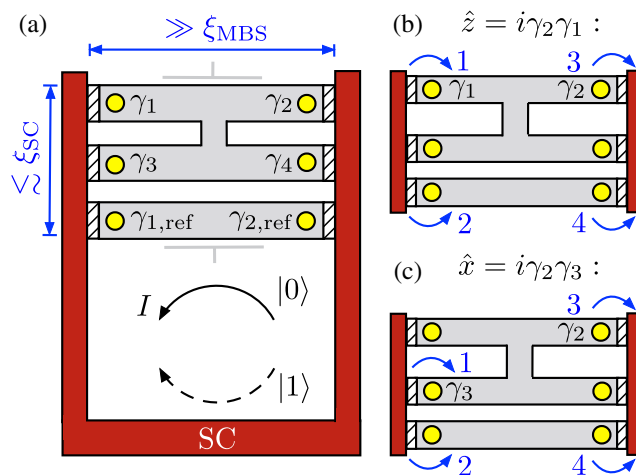


FIG. 1. (a) Minimal setup for a MSQ experiment. A four-terminal TSC island realizing a single MSQ and a two-terminal reference island (both gray) are placed in an s -wave SC Josephson junction (red). The horizontal extent of the islands are assumed to be larger than the localization length ξ_{MBS} of the MBSs γ_ℓ and $\gamma_{\ell,\text{ref}}$ (yellow), which emerge at the terminal points of the islands. The vertical extent of the unit cell is assumed to be at most of the order of the superconducting coherence length ξ_{SC} thereby enabling Cooper pair splitting between the superconducting leads mediated by the MBSs. With the suitable choice of tunnel couplings discussed in the text, the states of the MSQ, $|0\rangle$ and $|1\rangle$, can be readout by measuring the direction of the persistent Josephson current in a loop. (b) Typical Cooper pair splitting process between one of the four-terminal islands and the two-terminal reference islands utilized for implementing rotations around the z axis of the MSQ Bloch sphere. (c) Same as (a) but for rotations around the x axis of the MSQ Bloch sphere.

the total charge on the TSC island [18–20]. Second, since a MSQ is formed by two *topologically degenerate* states that are separated from the excited states by the TSC gap, leakage to noncomputational states, which is a common problem encountered in gate operations on weakly anharmonic transmon qubits, is strongly suppressed. Third, both gate operations and qubit readout are realized solely by tuning tunnel couplings between the TSC island and the superconducting leads, which can be turned on and off on demand through local gates as recently demonstrated in semiconductor based superconducting qubits [21–23]. Importantly, a specific set of tunnel couplings are to be turned on only during the gate operation and measurement. The ability of pinching off unwanted tunnel couplings allows us to address MSQ individually without cross-talk errors. This provides an advantage over flux-controlled tuning of Josephson energy in transmon and hybrid transmon-Majorana qubits [24].

The use of the superconducting interference effect for qubit manipulation and readout in our proposal constitutes a key advantage over other Majorana-based quantum computation platforms [18–20] where MBSs are addressed by Aharonov-Bohm interference of single electrons [25]. The latter requires electron phase coherence in a non-superconducting lead. The limited phase coherence length in InAs nanowires [26,27] places an important constraint on device geometries. In contrast, in our setup, there is no upper bound on the size of the superconducting loop, as the persistent supercurrent is dissipationless. Importantly, the separation between the two parallel TSC islands is required to be shorter than the superconducting coherence length, in order to enable Cooper pair splitting processes. For conventional superconductors such as aluminium, the coherence length can be several hundreds of nanometers [28]. Finally, another principal advantage of MSQs is that the energy gap of the SC leads provides additional protection against quasiparticle poisoning independent of the island charging energies. This feature should significantly reduce the need for fine-tuning of the island gate charges to warrant protection from quasiparticle poisoning.

Setup.—The setup for a minimal MSQ experiment enabling both single-qubit rotations and readout is depicted in Fig. 1(a). It comprises a single four-terminal island as well as a two-terminal reference island. The MBSs that form at the terminal points ℓ are denoted by γ_ℓ for the four-terminal island and by $\gamma_{\ell,\text{ref}}$ for the two-terminal reference island. We assume that the horizontal extent of the islands is much larger than the MBS localization length ξ_{MBS} such that the wave function hybridization of MBSs localized at opposite terminals is negligible and, therefore, all MBSs reside at zero energy. Since the TSC islands are of mesoscopic size, each island acquires a finite charging energy

$$U = (ne - Q)^2/2C, \quad (1a)$$

$$U_{\text{ref}} = (n_{\text{ref}}e - Q_{\text{ref}})^2/2C_{\text{ref}}. \quad (1b)$$

Here, n and n_{ref} denote the number of unit charges on the islands. Furthermore, Q and Q_{ref} are gate charges which are continuously tunable via gate voltages across capacitors with capacitances C and C_{ref} , respectively. For simplicity, we will focus on the case of equal capacitances, $C = C_{\text{ref}}$. Assuming the strong Coulomb blockade regime and a tuning of the gate charges Q , Q_{ref} close to integer values, the total fermion parities of the islands obey the constraints [25,29],

$$\gamma_1\gamma_2\gamma_3\gamma_4 = (-1)^{n_0+1}, \quad (2a)$$

$$i\gamma_{1,\text{ref}}\gamma_{2,\text{ref}} = (-1)^{n_{0,\text{ref}}}. \quad (2b)$$

In writing down these expressions, we have omitted finite-energy quasiparticle contributions, which is justified provided that the island energy gaps define the largest energy scale of the setup. A consequence of the constraints given in both Eqs. (2a) and (2b) is that the dimensionality of the ground state subspace at zero charging energy decreases by a factor of two for all islands. In particular, for the four-terminal island, the fourfold degenerate ground state subspace at zero charging energy reduces to a twofold degenerate ground state subspace which makes up the MSQ. The Pauli matrices acting on the each of the two MSQs are given by

$$\hat{x} = i\gamma_2\gamma_3, \quad \hat{y} = i\gamma_1\gamma_3, \quad \hat{z} = i\gamma_2\gamma_1. \quad (3)$$

As shown in Fig. 1(a), the TSC islands are placed in a Josephson junction of two bulk, s -wave SC leads $m = L, R$ and are used to address the MSQs through tunable tunnel couplings. The BCS (Bardeen-Cooper-Schrieffer) Hamiltonian of the SC leads is given by

$$H_0 = \sum_{m=L,R} \sum_{\mathbf{k}} \Psi_{m,\mathbf{k}}^\dagger (\xi_{\mathbf{k}}\eta_z + \Delta_m\eta_x e^{i\varphi_m\eta_z}) \Psi_{m,\mathbf{k}}, \quad (4)$$

where $\Psi_{m,\mathbf{k}} = (c_{m,\mathbf{k}\uparrow}, c_{m,-\mathbf{k}\downarrow}^\dagger)^T$ denotes a Nambu spinor with $c_{m,\mathbf{k}s}$ being the annihilation operator of an electron with momentum \mathbf{k} and Kramers index $s = \uparrow, \downarrow$. The magnitude and phase of the superconducting ordering parameter are given by Δ_m and φ_m , respectively. The Pauli matrices $\eta_{x,y,z}$ are acting in Nambu space. For simplicity, we will assume that the magnitudes of the SC order parameters are identical for both leads, $\Delta \equiv \Delta_m$.

The tunneling Hamiltonians which couple the SC leads to the MBSs at the terminal points are given by

$$H_T = \sum_{m,\ell} \sum_{\mathbf{k},s} \lambda_{m\ell}^s c_{m,\mathbf{k}s}^\dagger \gamma_\ell e^{-i\phi/2} + \text{H.c.}, \quad (5a)$$

$$H_{T,\text{ref}} = \sum_{m,\ell} \sum_{\mathbf{k},s} \lambda_{m\ell}^s c_{m,\mathbf{k}s}^\dagger \gamma_{\ell,\text{ref}} e^{-i\phi_{\text{ref}}/2} + \text{H.c.}, \quad (5b)$$

for the four-terminal and the two-terminal reference islands, respectively. For simplicity, the tunnel couplings are taken to be pointlike. This is justified provided that the separation between individual tunneling contacts is much smaller than the superconducting coherence length ξ_{SC} . In the subsequent discussions, we will assume that the lead electrons will only couple to nearby MBSs, i.e., $\lambda_{L2}^s = \lambda_{L4}^s = \lambda_{R1}^s = \lambda_{R3}^s = 0$ and $\lambda_{L2,\text{ref}}^s = \lambda_{R1,\text{ref}}^s = 0$. This is justified if the MBS localization length ξ_{MBS} is much larger than horizontal segments of the islands. The remaining nonzero tunnel couplings are assumed to take on the most general complex and spin-dependent form. Couplings of the lead fermions to finite energy quasiparticles are neglected, which is justified if the energy gap of the TSC islands is sufficiently large. Moreover, the operators $e^{\pm i\phi/2}$ and $e^{\pm i\phi_{\text{ref}}/2}$ increase or decrease the total charge of the four-terminal island or the two-terminal reference island by one charge unit, $[n, e^{\pm i\phi/2}] = \pm e^{\pm i\phi/2}$ and $[n_{\text{ref}}, e^{\pm i\phi_{\text{ref}}/2}] = \pm e^{\pm i\phi_{\text{ref}}/2}$, while the MBSs operators γ_ℓ and $\gamma_{\ell,\text{ref}}$ change the electron number parity of the respective islands [25]. In summary, the Hamiltonian for a minimal MSQ experiment is given by $H = H_0 + U + U_{\text{ref}} + H_T + H_{T,\text{ref}}$.

Single-qubit control.—In this section, we describe the simplest MSQ experiments which allows for both readout and manipulation of a single MSQ. In combination with the two-qubit entangling operation introduced in the next section, this will enable universal quantum computation [30].

First, we discuss rotations around the z axis of the MSQ Bloch sphere as well as the readout of the \hat{z} eigenvalue. We, therefore, consider the case when only the couplings to the two-terminal reference island and the two couplings λ_{L1}^s and λ_{R2}^s at opposite boundaries of the four-terminal island are nonvanishing; see Fig. 1(b).

In this case, second-order processes in which a Cooper pair tunnels between one of the SC leads and one of the TSC islands are prohibited as a result of conflicting pairing symmetries assuming that couplings to finite-energy quasiparticles are negligible [31–34]. Moreover, Cooper pair transport occurring separately between each SC lead and both TSC islands is also forbidden, since these processes change the charge of the TSC islands, and in this way leak out of the low-energy Hilbert space. Consequently, the Josephson coupling between the SC leads is mediated exclusively by fourth-order co-tunneling processes via both the two-terminal and the four-terminal island. An example of such a fourth-order process involves extracting two electrons which form a Cooper pair from one of the SC leads and placing them onto the two spatially separated islands in the first two intermediate steps. Such a coherent splitting of Cooper pairs requires the vertical distance of the islands to be smaller than the superconducting coherence length ξ_{SC} and leads to virtually excited states of order $U \equiv e^2/2C$ on both islands. In the final two intermediate

steps, the Cooper pair is recombined on the other lead, and the system thereby returns to its ground state.

The amplitudes of all Cooper pair splitting processes can be computed perturbatively in the weak-tunneling limit, $\pi\nu_m |\lambda_{m\ell,\text{ref}}^s \lambda_{m\ell}^s| \ll \Delta, U$ with ν_m the normal-state density of states per spin of the lead m at the Fermi energy. The results are summarized by an effective Hamiltonian acting on the BCS ground states of the leads and the charge ground states of the islands [35],

$$H_{z,\text{eff}} = (-1)^{n_{0,\text{ref}}+1} (J_{12} + \tilde{J}_{12}) \cos(\varphi + \varphi_{12}) \hat{z}, \quad (6)$$

where we have omitted contributions that are independent of the SC phase difference as they do not contribute to the Josephson current. Moreover, we have introduced the coupling constants and the anomalous phase shift,

$$\begin{aligned} J_{\ell\ell'} &= \frac{32|\Gamma_{L\ell}\Gamma_{R\ell'}|}{\pi^2\Delta} \int_1^\infty \frac{dx dy}{f(x)f(y)[f(x)+f(y)]g(x)g(y)}, \\ \tilde{J}_{\ell\ell'} &= \frac{64|\Gamma_{L\ell}\Gamma_{R\ell'}|}{\pi^2\Delta} \int_1^\infty \frac{dx dy}{f(x)f(y)[g(x)+g(y)]g(x)g(y)}, \\ \varphi_{\ell\ell'} &= \arg[\Gamma_{L\ell}^* \Gamma_{R\ell'}], \end{aligned} \quad (7)$$

with the functions $f(x) \equiv \sqrt{1+x^2}$, $g(x) \equiv \sqrt{1+x^2} + U/\Delta$ as well as the hybridization

$$\Gamma_{m\ell} \equiv \pi\nu_m (\lambda_{m\ell,\text{ref}}^\downarrow \lambda_{m\ell}^\uparrow - \lambda_{m\ell,\text{ref}}^\uparrow \lambda_{m\ell}^\downarrow). \quad (8)$$

The effective Hamiltonian given in Eq. (6) is the first main finding of our work. Three aspects are noteworthy:

(i) The unitary time-evolution operator of the effective Hamiltonian implements rotations around the z axis of the MSQ Bloch sphere. More explicitly, by pulsing the couplings and phases of the effective Hamiltonian for a time t_z such that $(-1)^{n_{0,\text{ref}}+1} \int^{t_z} [J_{12}(t) + \tilde{J}_{12}(t)] \cos[\varphi(t) + \varphi_{12}(t)] dt = \hbar\theta_z/2$ a rotation by an arbitrary angle θ_z around the z axis of the MSQ Bloch sphere is achieved.

(ii) A choice of basis for the MSQ is given by the eigenstates of the \hat{z} -Pauli operator. Thus, a readout of the MSQ in this basis amounts to measuring the eigenvalues $z = \pm 1$ of the \hat{z} -Pauli operator. This can be accomplished by measuring the sign of the resulting zero-temperature Josephson current,

$$I = \frac{2e}{\hbar} (-1)^{n_{0,\text{ref}}} (J_{12} + \tilde{J}_{12}) \sin(\varphi + \varphi_{12}) z. \quad (9)$$

For $n_{0,\text{ref}}$ being odd (even), a negative (positive) critical current implies that $z = +1$ while a positive (negative) critical currents implies that $z = -1$, see Fig. 1(a).

(iii) A necessary requirement for a nonzero effective Hamiltonian is that $\Gamma_{1L} \neq 0$ and $\Gamma_{2R} \neq 0$. These conditions are fulfilled granted that the MBSs in the two islands couple asymmetrically to the two spin species of the SC leads, see Eq. (8). In fact, the strength of the Josephson coupling is maximized if the MBSs in different islands couple to

opposite spin species in the SC leads. For parallel topological nanowires [19,20,36–41], there are multiple ways on how the desired asymmetry can be realized: One option is to have a common spin polarization in the two nanowires and a finite spin-orbit coupling in the tunneling barriers which rotates the spin [42]. By adjusting the tunneling barrier lengths, we can transport a Cooper pair across the junction by pure spin-flip tunneling in the barriers to the reference island and pure normal tunneling in the barriers to the four-terminal island. An alternative option is to generate different (ideally opposite) spin polarization in the two nanowires by using local magnetic fields. Such fields could be obtained by coating the wires with ferromagnets that produce different exchange fields.

So far, we have focused on rotations around the z axis of the MSQ Bloch sphere. We will now show that rotations around the x axis can be realized similarly. To this end, we choose λ_{3L}^s , λ_{2R}^s , $\lambda_{1,\text{ref}}^s$ and $\lambda_{2,\text{ref}}^s$ as the only nonzero tunnel couplings, see Fig. 1(c). The Josephson coupling between the superconducting leads is again facilitated solely by Cooper pair splitting processes via the TSC islands. In the weak tunneling limit, the amplitudes of these processes are summarized by an effective Hamiltonian acting on the BCS ground states of the leads and the charge ground states of the islands [35],

$$H_{x,\text{eff}} = (-1)^{n_{0,\text{ref}}+1} (J_{32} + \tilde{J}_{32}) \cos(\varphi + \varphi_{32}) \hat{x}. \quad (10)$$

It is not hard to see that pulsing the couplings and phases of this effective Hamiltonian for a time t_x such that $(-1)^{n_{0,\text{ref}}+1} \int^{t_x} [J_{32}(t) + \tilde{J}_{32}(t)] \cos[\varphi(t) + \varphi_{32}(t)] dt = \hbar\theta_x/2$ enables rotations by an angle θ_x around the x axis of the MSQ Bloch sphere. Combining this observation with the results of Eq. (6) allows us to perform rotations around two independent axes on the Bloch sphere and, therefore, enables the implementation of arbitrary single-qubit gates acting on the MSQ.

Two-qubit gates.—What remains to be shown to achieve universality in our setup is the implementation of a two-qubit entangling gate. This will be the topic of the present section. As a starting point, we consider two four-terminal islands labeled by $j = a, b$ and choose $\lambda_{3L,a}^s$, $\lambda_{2R,a}^s$, $\lambda_{3L,b}^s$, $\lambda_{2R,b}^s$ as the only nonzero tunnel couplings, see Fig. 2(a). The Cooper pair splitting processes which lead to a Josephson coupling between the superconducting leads are now entirely facilitated by the two four-terminal TSC islands. Their amplitudes can be computed in the weak-tunneling limit, $\pi\nu_m |\lambda_{m\ell}^s, \lambda_{m\ell'}^s| \ll \Delta, U$, and are summarized by an effective Hamiltonian which acts on the BCS ground states and the charge ground states of the TSC islands [35],

$$H_{\text{eff}} = (J + \tilde{J}) \cos(\varphi + \varphi_0) \hat{x}_a \hat{x}_b. \quad (11)$$

Here, we have introduced the couplings constants and the anomalous phase shift,

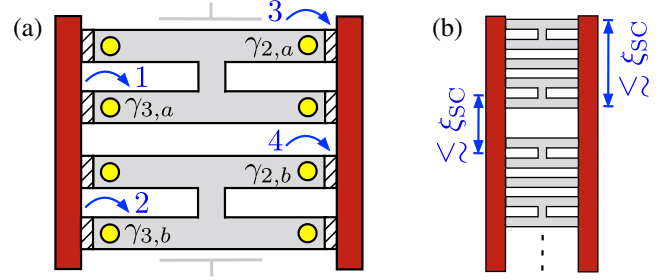


FIG. 2. (a) Typical Cooper pair splitting process between two four-terminal islands implementing a two-qubit entangling $XX_\chi \equiv \exp(-i\chi\hat{x}_a\hat{x}_b)$ gate for some parameter χ . (b) Linear array of unit cells. To maximize the critical current and, thereby, optimize qubit measurement times, the vertical extent of each unit cell is of the order of the SC coherence length ξ_{SC} . Neighboring unit cells are also separated by a distance $\lesssim \xi_{\text{SC}}$ to allow for coherent exchange of quantum information via SWAP gates.

$$J = \frac{32|\Gamma'_{L3}\Gamma'_{R2}|}{\pi^2\Delta} \int_1^\infty \frac{dxdy}{f(x)f(y)[f(x)+f(y)]g(x)g(y)},$$

$$\tilde{J} = \frac{64|\Gamma'_{L3}\Gamma'_{R2}|}{\pi^2\Delta} \int_1^\infty \frac{dxdy}{f(x)f(y)[g(x)+g(y)]g(x)g(y)},$$

$$\varphi_0 = \arg[(\Gamma'_{L3})^*\Gamma'_{R2}]. \quad (12)$$

Moreover, we have defined the hybridization

$$\Gamma'_{m\ell} \equiv \pi\nu_m (\lambda_{m\ell,b}^\downarrow \lambda_{m\ell,a}^\uparrow - \lambda_{m\ell,b}^\uparrow \lambda_{m\ell,a}^\downarrow). \quad (13)$$

The effective Hamiltonian in Eq. (11) is the second main result of our work. By pulsing the couplings and phases for a time τ such that $\int^\tau [J(t) + \tilde{J}(t)] \cos[\varphi(t) + \varphi_0(t)] dt = \hbar\chi$, the unitary time-evolution operator of the effective Hamiltonian implements an $XX_\chi \equiv \exp(-i\chi\hat{x}_a\hat{x}_b)$ gate for some parameter χ . It is well known in the literature that the $XX_{\pi/4}$ gate together single-qubit operations implements a CNOT gate [43],

$$\text{CNOT} = X_{-\pi/2,b} Y_{-\pi/2,a} X_{-\pi/2,a} XX_{\pi/4} Y_{\pi/2,a}, \quad (14)$$

where we have introduced the single-qubit gates $X_{\theta,j} \equiv \exp(-i\theta\hat{x}_j/2)$ and $Y_{\theta,j} \equiv \exp(-i\theta\hat{y}_j/2)$ with some parameter θ . We note that the CNOT gate defined in Eq. (14) uses the MSQ a as control and the MSQ b as target. A CNOT' gate in which the roles of control and target qubit are reversed can readily be obtained by applying single-qubit Hadamard gates, $\text{CNOT}' = H_a H_b \text{CNOT} H_a H_b$ with $H_\ell = (\hat{x}_\ell + \hat{z}_\ell)/\sqrt{2}$. In conclusion, the combination of the single-qubit gates introduced in the previous section together with the two-qubit CNOT gate is sufficient for universal quantum computation with MSQs.

To assemble a scalable MSQ computer, we consider unit cells comprised of two four-terminal islands and a single reference island. This enables the implementation of a

universal gate set comprised of arbitrary single-qubit gates and a two-qubit entangling gate within each unit cell. Importantly, such a unit cell can readily be scaled to a linear array of multiple unit cells as depicted in Fig. 2(b). The distance between the individual unit cells in such an array is taken to be at most of the order of the superconducting coherence length ξ_{SC} . The coherent exchange of quantum information between different unit cells is facilitated by SWAP gates acting on MSQs of neighboring unit cells [35].

Before closing, we envision two candidate platforms for a material realization of MSQs. The first platform is topologically SC nanowires [36–41]. Here, we define the SC islands by locally etching the mesoscopic SC that is deposited on the nanowires. This creates semiconducting tunneling barriers with transparencies that are tunable by local side gates [44–46]. It is worth mentioning that Cooper-pair splitting between parallel semiconducting nanowires coupled to a common superconducting electrode—the key ingredient of our proposal—has been observed in recent experiments [47]. The second platform that we envision for a MSQ realization is TSC islands defined in a heterostructure of a two-dimensional electron gas and a SC by means of top-down lithography and gating [48]. A key advantage of these devices is that they may enable rapid scaling from a single MSQ to the multi-MSQ architectures of Fig. 2(b).

Conclusions.—We have proposed a platform for universal quantum computation realized by conventional SC leads addressing MSQs formed by the charge ground states of four-terminal TSC islands. We have shown how Cooper pair splitting enables single-qubit operations, qubit readout, as well as two-qubit entangling gates. Hence, our platform may provide an alternative approach to superconducting quantum computation.

We would like to thank Morten Kjaergaard for helpful discussions. This work was supported by DOE Office of Basic Energy Sciences, Division of Materials Sciences and Engineering under Award No. DE-SC0019275 (development of next generation qubits) and benefited from Award No. DE-SC0010526 (core research of L. F.). Work of C. S. was supported in part by the Swiss SNF under Project No. 174980.

[1] H. Paik, D. I. Schuster, L. S. Bishop, G. Kirchmair, G. Catelani, A. P. Sears, B. R. Johnson, M. J. Reagor, L. Frunzio, L. I. Glazman, S. M. Girvin, M. H. Devoret, and R. J. Schoelkopf, *Phys. Rev. Lett.* **107**, 240501 (2011).
 [2] C. Rigetti, J. M. Gambetta, S. Poletto, B. L. T. Plourde, J. M. Chow, A. D. Córcoles, J. A. Smolin, S. T. Merkel, J. R. Rozen, G. A. Keefe, M. B. Rothwell, M. B. Ketchen, and M. Steffen, *Phys. Rev. B* **86**, 100506 (2012).
 [3] J. B. Chang, M. R. Vissers, A. D. Corcoles, M. Sandberg, J. Gao, D. W. Abraham, J. M. Chow, J. M. Gambetta,

M. B. Rothwell, G. A. Keefe, M. Steffen, and D. P. Pappas, *Appl. Phys. Lett.* **103**, 012602 (2013).
 [4] R. Barends *et al.*, *Nature (London)* **508**, 500 (2014).
 [5] S. Sheldon, E. Magesan, J. M. Chow, and J. M. Gambetta, *Phys. Rev. A* **93**, 060302 (2016).
 [6] F. Helmer, M. Mariani, A. G. Fowler, J. von Delft, E. Solano, and F. Marquardt, *Europhys. Lett.* **85**, 50007 (2009).
 [7] D. P. DiVincenzo, *Phys. Scr.* **2009**, 014020 (2009).
 [8] A. G. Fowler, M. Mariani, J. M. Martinis, and A. N. Cleland, *Phys. Rev. A* **86**, 032324 (2012).
 [9] A. D. Corcoles, E. Magesan, S. J. Srinivasan, A. W. Cross, M. Steffen, J. M. Gambetta, and J. M. Chow, *Nat. Commun.* **6**, 6979 (2015).
 [10] M. Takita, A. D. Córcoles, E. Magesan, B. Abdo, M. Brink, A. Cross, J. M. Chow, and J. M. Gambetta, *Phys. Rev. Lett.* **117**, 210505 (2016).
 [11] J. Kelly *et al.*, *Nature (London)* **519**, 66 (2015).
 [12] J. M. Gambetta, A. D. Córcoles, S. T. Merkel, B. R. Johnson, J. A. Smolin, J. M. Chow, C. A. Ryan, C. Rigetti, S. Poletto, T. A. Ohki, M. B. Ketchen, and M. Steffen, *Phys. Rev. Lett.* **109**, 240504 (2012).
 [13] O.-P. Saira, J. P. Groen, J. Cramer, M. Meretska, G. de Lange, and L. DiCarlo, *Phys. Rev. Lett.* **112**, 070502 (2014).
 [14] J. Z. Blumoff, K. Chou, C. Shen, M. Reagor, C. Axline, R. T. Brierley, M. P. Silveri, C. Wang, B. Vlastakis, S. E. Nigg, L. Frunzio, M. H. Devoret, L. Jiang, S. M. Girvin, and R. J. Schoelkopf, *Phys. Rev. X* **6**, 031041 (2016).
 [15] A. Kringhøj, L. Casparis, M. Hell, T. W. Larsen, F. Kuemmeth, M. Leijnse, K. Flensberg, P. Krogstrup, J. Nygård, K. D. Petersson, and C. M. Marcus, *Phys. Rev. B* **97**, 060508 (2018).
 [16] M. D. Hutchings, J. B. Hertzberg, Y. Liu, N. T. Bronn, G. A. Keefe, J. M. Chow, and B. L. T. Plourde, *Phys. Rev. Applied* **8**, 044003 (2017).
 [17] A. Y. Kitaev, *Phys. Usp.* **44**, 131 (2001).
 [18] S. Vijay and L. Fu, *Phys. Rev. B* **94**, 235446 (2016).
 [19] S. Plugge, A. Rasmussen, R. Egger, and K. Flensberg, *New J. Phys.* **19**, 012001 (2017).
 [20] T. Karzig, C. Knapp, R. M. Lutchyn, P. Bonderson, M. B. Hastings, C. Nayak, J. Alicea, K. Flensberg, S. Plugge, Y. Oreg, C. M. Marcus, and M. H. Freedman, *Phys. Rev. B* **95**, 235305 (2017).
 [21] G. de Lange, B. van Heck, A. Bruno, D. J. van Woerkom, A. Geresdi, S. R. Plissard, E. P. A. M. Bakkers, A. R. Akhmerov, and L. DiCarlo, *Phys. Rev. Lett.* **115**, 127002 (2015).
 [22] T. W. Larsen, K. D. Petersson, F. Kuemmeth, T. S. Jespersen, P. Krogstrup, J. Nygård, and C. M. Marcus, *Phys. Rev. Lett.* **115**, 127001 (2015).
 [23] L. Casparis, M. R. Connolly, M. Kjaergaard, N. J. Pearson, A. Kringhøj, T. W. Larsen, F. Kuemmeth, T. Wang, C. Thomas, S. Gronin, G. C. Gardner, M. J. Manfra, C. M. Marcus, and K. D. Petersson, *Nat. Nanotechnol.* **13**, 915 (2018).
 [24] T. Hyart, B. van Heck, I. C. Fulga, M. Burrello, A. R. Akhmerov, and C. W. J. Beenakker, *Phys. Rev. B* **88**, 035121 (2013).
 [25] L. Fu, *Phys. Rev. Lett.* **104**, 056402 (2010).

- [26] D. Liang, M. R. Sakr, and X. P. A. Gao, *Nano Lett.* **9**, 1709 (2009).
- [27] Y.-J. Doh, A. L. Roest, E. P. A. M. Bakkers, S. De Franceschi, and L. P. Kouwenhoven, *J. Korean Phys. Soc.* **54**, 135 (2009).
- [28] M. Cyrot and D. Pavuna, *Introduction to Superconductivity and High- T_c Materials* (World Scientific Publishing Co. Pte. Ltd., Singapore, 1992), p. 38.
- [29] C. Xu and L. Fu, *Phys. Rev. B* **81**, 134435 (2010).
- [30] J.-L. Brylinski and R. Brylinski, [arXiv:quant-ph/0108062](https://arxiv.org/abs/quant-ph/0108062).
- [31] A. Zazunov and R. Egger, *Phys. Rev. B* **85**, 104514 (2012).
- [32] A. Zazunov, R. Egger, M. Alvarado, and A. L. Yeyati, *Phys. Rev. B* **96**, 024516 (2017).
- [33] A. Zazunov, A. Iks, M. Alvarado, A. L. Yeyati, and R. Egger, [arXiv:1801.10343](https://arxiv.org/abs/1801.10343).
- [34] C. Schrade and L. Fu, *Phys. Rev. Lett.* **120**, 267002 (2018).
- [35] See Supplemental Material at <http://link.aps.org/supplemental/10.1103/PhysRevLett.121.267002> for more details on the derivation of the effective Hamiltonians used for the implementation of the single-qubit and the two-qubit gates.
- [36] V. Mourik, K. Zuo, S. M. Frolov, S. R. Plissard, E. P. A. M. Bakkers, and L. P. Kouwenhoven, *Science* **336**, 1003 (2012).
- [37] A. Das, Y. Ronen, Y. Most, Y. Oreg, M. Heiblum, and H. Shtrikman, *Nat. Phys.* **8**, 887 (2012).
- [38] H. O. H. Churchill, V. Fatemi, K. Grove-Rasmussen, M. T. Deng, P. Caroff, H. Q. Xu, and C. M. Marcus, *Phys. Rev. B* **87**, 241401(R) (2013).
- [39] S. Gazibegovic *et al.*, *Nature (London)* **548**, 434 (2017).
- [40] S. Vaitiekėnas, A. M. Whiticar, M. T. Deng, F. Krizek, J. E. Sestoft, S. Marti-Sanchez, J. Arbiol, P. Krogstrup, L. Casparis, and C. M. Marcus, *Phys. Rev. Lett.* **121**, 147701 (2018).
- [41] F. Krizek, J. E. Sestoft, P. Aseev, S. Marti-Sanchez, S. Vaitiekėnas, L. Casparis, S. A. Khan, Y. Liu, T. Stankevic, A. M. Whiticar, A. Fursina, F. Boekhout, R. Koops, E. Uccelli, L. P. Kouwenhoven, C. M. Marcus, J. Arbiol, and P. Krogstrup, *Phys. Rev. Mater.* **2**, 093401 (2018).
- [42] D. Bercioux and P. Lucignano, *Rep. Prog. Phys.* **78**, 106001 (2015).
- [43] D. Maslov, *New J. Phys.* **19**, 023035 (2017).
- [44] F. Nichele, A. C. C. Drachmann, A. M. Whiticar, E. C. T. O'Farrell, H. J. Suominen, A. Fornieri, T. Wang, G. C. Gardner, C. Thomas, A. T. Hatke, P. Krogstrup, M. J. Manfra, K. Flensberg, and C. M. Marcus, *Phys. Rev. Lett.* **119**, 136803 (2017).
- [45] H. Zhang *et al.*, *Nature (London)* **556**, 74 (2018).
- [46] J. van Veen, A. Proutski, T. Karzig, D. I. Pikulin, R. M. Lutchyn, J. Nygård, P. Krogstrup, A. Geresdi, L. P. Kouwenhoven, and J. D. Watson, *Phys. Rev. B* **98**, 174502 (2018).
- [47] S. Baba, C. Jünger, S. Matsuo, A. Baumgartner, Y. Sato, H. Kamata, K. Li, S. Jeppesen, L. Samuelson, H. Xu, C. Schönenberger, and S. Tarucha, *New J. Phys.* **20**, 063021 (2018).
- [48] H. J. Suominen, M. Kjaergaard, A. R. Hamilton, J. Shabani, C. J. Palmstrøm, C. M. Marcus, and F. Nichele, *Phys. Rev. Lett.* **119**, 176805 (2017).